ORIGINAL ARTICLE

Tethered platelet capture provides a mechanism for restricting circulating platelet activation to the wound site

Irina D. Pokrovskaya MS[1] | Sung W. Rhee PhD[2] | Kelly K. Ball MS[1,2] | Jeffrey A. Kamykowski MS[1] | Oliver S. Zhao BS[3] | Denzel R. D. Cruz BS[3] | Joshua Cohen BS[3] | Maria A. Aronova PhD[3] | Richard D. Leapman PhD[3] | Brian Storrie PhD[1]

[1]Department of Physiology and Cell Biology, University of Arkansas for Medical Sciences, Little Rock, Arkansas, USA

[2]Department of Pharmacology and Toxicology, University of Arkansas for Medical Sciences, Little Rock, Arkansas, USA

[3]Laboratory of Cellular Imaging and Macromolecular Biophysics, National Institute of Biomedical Imaging and Bioengineering, National Institutes of Health, Bethesda, Maryland, USA

Correspondence
Brian Storrie, Department of Physiology and Cell Biology, University of Arkansas for Medical Sciences, 4301 West Markham Street, Little Rock, AR 72205, USA.
Email: StorrieBrian@uams.edu

Funding information
National Institutes of Health; Grant/Award Numbers: R01 HL119393, R56 HL119393, R01 155519, P01 HL146373, P01 HL040387, P01 HL120846

Handling Editor: Prof Yotis Senis

Abstract

Background: Puncture wounding is a longstanding challenge to human health for which understanding is limited, in part, by a lack of detailed morphological data on how the circulating platelet capture to the vessel matrix leads to sustained, self-limiting platelet accumulation.

Objectives: The objective of this study was to produce a paradigm for self-limiting thrombus growth in a mouse jugular vein model.

Methods: Data mining of advanced electron microscopy images was performed from authors' laboratories.

Results: Wide-area transmission electron mcrographs revealed initial platelet capture to the exposed adventitia resulted in localized patches of degranulated, procoagulant-like platelets. Platelet activation to a procoagulant state was sensitive to dabigatran, a direct-acting PAR receptor inhibitor, but not to cangrelor, a $P2Y_{12}$ receptor inhibitor. Subsequent thrombus growth was sensitive to both cangrelor and dabigatran and sustained by the capture of discoid platelet strings first to collagen-anchored platelets and later to loosely adherent peripheral platelets. Spatial examination indicated that staged platelet activation resulted in a discoid platelet tethering zone that was pushed progressively outward as platelets converted from one activation state to another. As thrombus growth slowed, discoid platelet recruitment became rare and loosely adherent intravascular platelets failed to convert to tightly adherent platelets.

Conclusions: In summary, the data support a model that we term Capture and Activate, in which the initial high platelet activation is directly linked to the exposed adventitia, all subsequent tethering of discoid platelets is to loosely adherent platelets that convert to tightly adherent platelets, and self-limiting, intravascular platelet activation over time is the result of decreased signaling intensity.

Essentials

- Ultrastructure shows that puncture bleeding cessation is by capping rather than plugging the hole.
- Platelet recruitment to a puncture must occur without endangering the circulating platelet activation.
- High-resolution electron micrographs reveal that platelets activate following tethering to wound.
- Decreased platelet tethering with weakened signaling provides a way to self-limit thrombus growth.

1 | INTRODUCTION

Vascular trauma presents in many forms from luminal disruptions to full breaches of the vessel wall. One major case is the puncture wound, a longstanding challenge to human health. In this example, the exposure of vessel wall extracellular matrix proteins—for instance, collagen—leads to platelet anchoring to the exposed adventitia in the case of a vein or externa in the case of an artery. Subsequent platelet binding to the matrix-anchored platelets leads to the formation of platelet aggregates that have recently been termed pedestals and columns and leads to beading cessation by extravascular capping of the puncture hole [1]. The exact activation state of the newly recruited platelets, ie, how closely these platelets resemble the circulating platelets and to what platelet activation state the subsequent rounds of platelet capture produce is presently unknown owing to the lack of detailed ultrastructural data over volumes that are near millimeter dimension. Moreover, what the effects of major antiplatelet drugs, such as $P2Y_{12}$ receptor inhibitors such as cangrelor [2], or direct oral anticoagulant (DOAC) drugs, such as dabigatran [3], are on specific platelet activation states is difficult to assess without such a detailed knowledge.

Here, we take the "big data" image sets generated by our laboratories [1] and analyze them at a high resolution to solve points central to the pathway of thrombus formation *in vivo*. Previously, we had binned the data and used it at a relatively low resolution to establish vaulted thrombus formation in a jugular vein puncture wound model [1]. Now, using the existing data sets, we shift our analytical efforts to key, high-resolution data contained within the 3-nm XY pixel size imaging of the midthrombus cross sections by using wide-area transmission electron microscopy (WA-TEM) [1]. These data are then supported by the unbiased data sets of full thrombus volumes from serial block face scanning electron microscopy (SBF-SEM) [1]. Data mining these mouse animal model data sets strongly indicate that all platelet activation processes in the formation of a puncture wound thrombus occur after platelet capture to the growing thrombus, ie, either at the surface or within the interior of thrombus itself. $P2Y_{12}$ and antithrombin inhibitor effects suggest that puncture wound thrombus growth is controlled early by multiple signaling multiple pathways acting in parallel and is likely self-limiting owing to decreased signaling intensity as the thrombus growth slows. We suggest that our data indicate a need for rethinking the mechanism(s) by which these drugs affect thrombus growth and the paradigms through which thrombus formation is conceptualized.

# 2 | MATERIALS AND METHODS

2.1 | Data mining

The analytical outcomes presented here—primarily at a high-zoom resolution, at 3.185 nm for WA-TEM or at 20- or 100-nm XY pixel size for SBF-SEM image sets—are mostly of images collected previously by the investigators' laboratories [1]. Raw image sets were deposited in the Electron Microscopy Public Image Archive (EMPLAR ID (accession code) 10785) in September 2021. The cangrelor sample electron microscopy was more recently performed and is not included in the deposited data sets. Any not previously deposited raw data are available on request to the corresponding author and will also be made available through the image repository. All image frames were derived at a unique zoom of the original image sets appropriate for revealing important features within the image data. The supporting laboratory bench methods have been published previously in an open access study [1]. Hence, we present only the essence of the bench laboratory methodology.

2.2 | Mice and reagents

All animal usage protocols were approved by the Institutional Animal Care and Use Committee. In total, 8- to 12-week-old, wild-type male and female C57BL/6 mice were used in equal numbers across the individual experimental time sets. All reagents have been cited previously [1–5].

2.3 | Drug treatments

The $P2Y_{12}$ inhibitor, cangrelor [2], was infused as an initial bolus dose of 0.3 mg/kg followed by 0.1 mg/kg/min maintenance with a syringe pump using a jugular venous catheter [1,4]. Dabigatran was injected
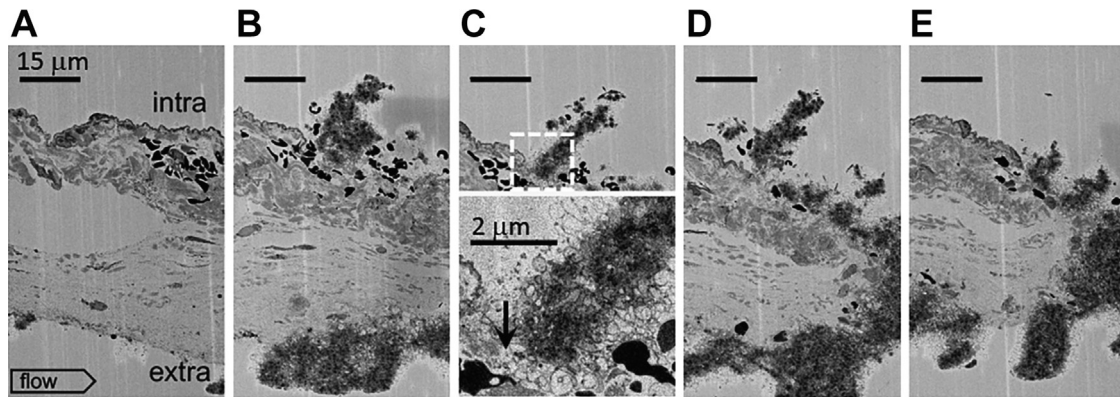
FIGURE 1 1-minute thrombus formation in response to a small scratch in the jugular vein endothelial cell layer exposing the collagen-rich adventitia to the lumen of the blood vessel. A-E. sequential ortho block face views, spaced 20 μm in Z, 20 nm XY raw pixel size, across a ∼60 μm wide scratch in the endothelial layer of the mouse jugular vein. As shown in B, C, D, and E, a columnar accumulation of platelets fills the damaged area. At its intravascular tip, the column is marked by discoid platelets (C). Furthermore, as shown in a zoom of the dotted square in C, the platelet column is at its base (arrow, C') and sides rich in procoagulant-like platelets nearly devoid of cytoplasm. The scratch is presumably the results of a needle slip and is distal from any puncture hole. Intravascular (top), extravascular (bottom), flow: left to right. A total of four 1-minute point samples were performed for SBF-SEM. In addition, 20 nm XY images were taken every 20 mm across the full thrombus width.

into the jugular vein at a bolus dose of 150 μg/kg, 20 minutes before puncture [1].

2.4 | Thrombus preparation and imaging

Jugular vein wounding was with a 30-gauge needle, 300-μm diameter nominal wound size, and thrombi were fixed *in situ* at 1 minute, 5 minutes, and 20 minutes with 4% paraformaldehyde and further processed for WA-TEM or SBF-SEM [1].

For WA-TEM, uranyl and lead citrate stainings were after embedding [1,6]. Automated montaged images were collected at the 3.185-nm XY pixel size using SerialEM software (version 3.6, 32-bit, University of Colorado, Boulder, CO) and routinely visualized with 3DMOD software (version 4.9.13, Mastronade group, University of Colorado, Boulder, CO). Fine image blending was performed with eTomo software (version 4.11.12, Mastronade Group, University of Colorado, CO).

For SBF-SEM, samples were stained with osmium, uranyl, and lead preembedding. Segmentation and data analysis were performed as described [1,5,7–9]. Volumes were computed by summating voxels within the segmented objects [1,5,7–9]. The imaged thrombi were rendered in the following color scheme: vessel wall (blue), tightly adherent platelets (green), loosely adherent platelets (yellow), degranulated platelets (orange), and red blood cells (red).

## 2.5 | Image visualization, statistics, and reproducibility

Image visualization was performed with IMOD software (version 4.11), a freeware product available from the Mastronade group, University of Colorado, Boulder, CO. iMac Pro computers (MacOs

10.14, 5K display) were used, and images were displayed at various zoom factors that ranged from 2% to 100% zoom of the raw images, themselves as large as 130,000 by 90,000 pixels. Volumetric image analysis of the data sets was performed as previously described [1,8], and the statistical significance of the outcomes was assessed by using the Student *t*-tests or, when appropriate, one-way ANOVA *post hoc* Bonferroni *t*-tests implemented in GraphPad Prism 5 [1]. Most experiments were reproduced by imaging at least 3 independent thrombi for each of the tested time interval. WA-TEM and SBF-SEM data provided independent ultrastructural approaches for each time interval [1].

3 | RESULTS

3.1 | Localized tethering of discoid-shaped platelets generates assembly patches that drive thrombus propagation

Initially, 1-minute after puncture SBF-SEM images taken at the 20-nm XY raw pixel size were used to probe for early steps in circulating platelet capture to a jugular puncture wound, 300 μm nominal diameter [1]. Unexpectedly, these images sometimes included non-puncture, needle damage to the adjacent endothelial cell layer. Consistent with our previous work showing the formation of platelet-rich pedestals and columns anchored to exposed collagen within the puncture hole or extravascular vessel wall [1], we observed a narrow column of platelets extending upward from the exposed adventitia into the intravascular lumen (Figure 1, flow left to right, individual frames, A-E, separated by the 20-μm Z step size). At the tip of the column, platelets retained some discoid features (frame C) as expected for platelets newly recruited from the vasculature. Below, platelets were more rounded. An approximately 2 to 3 platelet thick
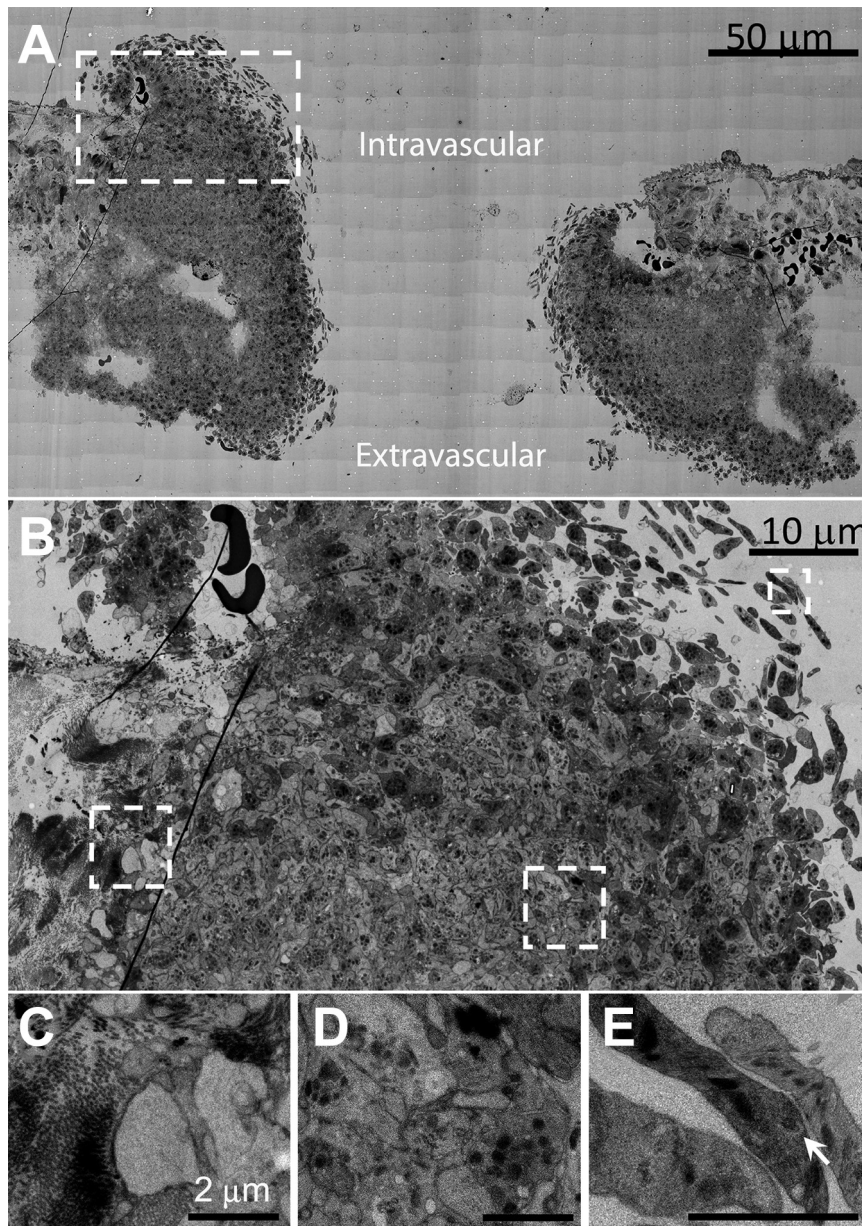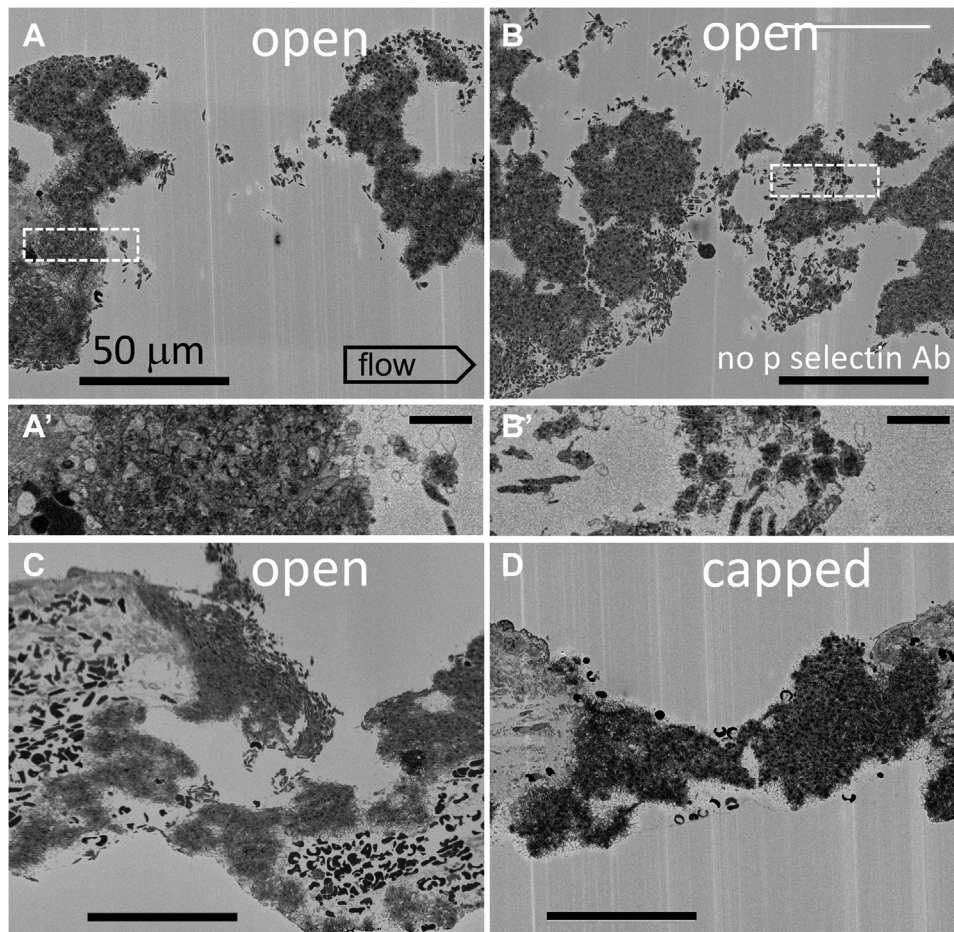
FIGURE 2 A 1-minute mouse jugular vein puncture wound thrombus showing both intravascular and extravascular areas of peripheral, discoid platelet recruitment to a forming thrombus. A. Montaged WA-TEM electron micrographs taken at 3.185 nm raw XY pixel size across the full puncture wound width, mid-puncture hole, and low image zoom. B. Image taken from left side of (A) (left side, upper, dashed box) showing at a higher zoom a full width image of one side of the thrombus from anchoring to collagen (left) to the recruitment of discoid platelets within the puncture hole. C. A high-zoom image taken from right side of B) (dashed box) showing the appearance of platelets at the platelet/exposed collagen-rich adventitia interface. These platelets appear nearly devoid of cytoplasm and procoagulant-like platelets. Note that collagen presents as bundles of fibers. These bundles are sometimes perpendicular (end on) to the platelets and sometimes parallel to the platelets. The collagen bundling results in the adventitia being a highly heterogeneous in its presentation to any locally adherent, ie, anchored platelets. D. High zoom, mid-thrombus example. Note the presence of α-granules. E. A high-zoom, hole peripheral image of newly captured discoid platelets. Arrow points to an example dense granule. A total of three 5-minute point samples were performed for WA-TEM. In addition, 3.185 nm XY images were at 3 separate depths across the full thrombus width.

layer of degranulated platelets was seen at the base of the column and lining the sides of the column (arrow, frame C'). Significantly, the images presented are the first example of the platelet column formation outside of a vessel puncture hole to the best of our knowledge.

To define the role of the apparent discoid-shaped platelets observed above as intermediates in platelet recruitment from the circulation, we turned to samples prepared for the higher resolution technique of WA-TEM (3-nm raw pixel size) and chose to concentrate on open, approximately midpuncture wound examples. We reasoned that these should provide images of abundant platelet recruitment examples (Figure 2, representative example, cut perpendicular to flow, n = 4) [1]. As shown in Figure 2A, an uncapped, ie, open, still bleeding, 1-minute thrombus consisted mostly of darkly staining, tightly packed, granulated platelets (Figure 2A, B, and Supplementary Figure 1). At 5% zoom, the occurrence of clusters of loosely held, peripheral,

discoid-shaped platelets, and discoid platelet strings (Figure 2A) were evident on both the intravascular and extravascular sides of the puncture hole and within the hole. Significantly, these thin-sectioned platelets contained numerous, dark granule profiles indicative of α-granules, a distinctive property of circulating platelets (20% zoom Figure 2B, 40% zoom Figure 2C, D, 75% zoom Figure 2E, and full page figure Supplementary Figure 1). These discoid platelets appeared to be tethered to the thrombus with platelets distal as much as 3 to 5 μm from the main body of the thrombus and the closest gap between discoid platelets of 30 to 50 nm (Supplementary Figure 1). As expected for nonactivated platelets, the discoid-shaped platelets contained rare examples of dense granules (Figure 2E, arrowhead). Dense granule examples are expected to be rare in thin sections because the number of dense granules per mouse platelet in full 3D rendering is low 2.1, 10-fold fewer than α-granules [10].

FIGURE 3 Single-slice, SBF-SEM, 1-minute thrombus images (20 nm XY raw pixel size) from four separate examples (A, B, C, and D) within a jugular vein, puncture hole showing peripheral, discoid-shaped platelet recruitment on both intravascular and extravascular surfaces of open, but not capped puncture wounds. A', B' show the platelet appearance of dashed box areas at a 2× higher zoom. In addition, 20 nm pixel size image slices are taken every 20 μm across the thrombus. Intravascular (top) and extravascular (bottom of frame). A total of four 1-minute point samples were performed for SBF-SEM. The examples shown are at full cross shown at approximately mid-thrombus depth.

Progressive and distinctive transitions of the platelets from discoid to rounded and tightly packed morphology were obvious (Figure 2B–E, Supplementary Figure 1). In net, we observed sequential differentiation in platelet morphology that suggests an ordered progression from discoid-like, putative circulating platelets distally tethered to the thrombus consistent with the action of a long extended molecule such as VWF, as previously discussed, eg, [11,12] to tighter platelet packing through relatively short molecular associations likely mediated by integrins and fibrinogen [12–14]. These images are suggestive that circulating platelets during thrombus growth (ie, propagation) are "reeled in" by a tethering process, ie, a "fishing line." As shown in Figure 2B, C, the collagen-rich, vessel adventitia/platelet interface lining the inner periphery of the thrombus was distinct. Here a fully degranulated, cytosol-free, interfacial layer of the platelets can be seen to vary over a thickness of between 1 and 4 platelets corresponding to a thickness of 1 to 3 μm. One probable high activation signal here is adventitial protein interactions, for example, with platelet GPVI receptor [15,16]. Others include VWF interactions. Overall, the data indicate that any adventitial signaling extends out only a micrometer, ie, a few platelet diameters.

To test spatial localization of discoid platelet recruitment within the growing thrombus, we turned to the unbiased sampling technique of SBF-SEM from which full spatially rendered thrombus modeling can be performed. As shown in the representative image slices, 20-nm raw pixel size, of the 4 individual, 1-minute after puncture thrombi acquired in the midhole region, it is evident that there are multiple discoid platelet-rich, local patches, ie, assembly patches along the intravascularly exposed surface areas of the forming thrombus and the extravascular surfaces of the open wound cavities (Figure 3A–C, A', B' zooms of boxed areas in A, B). In the fully capped puncture hole, where no further bleeding occurs, discoid platelets characteristic of assembly patches were present only on intravascular, flow-accessible, thrombus surfaces (Figure 3D vs A–C). Again, the discoid platelets were distal, ie, tethered. On a global scale as rendered across full thrombus volumes from thousands of micrographs acquired with a 100-nm pixel size, 1-minute thrombi displayed localized patches of loosely packed, adherent platelets on the exposed surfaces of open wound thrombi but not on the extravascular surface of a closed, capped thrombus (Figure 4). We suggest that assembly patches must be short lived as inferred from the rapid disappearance of
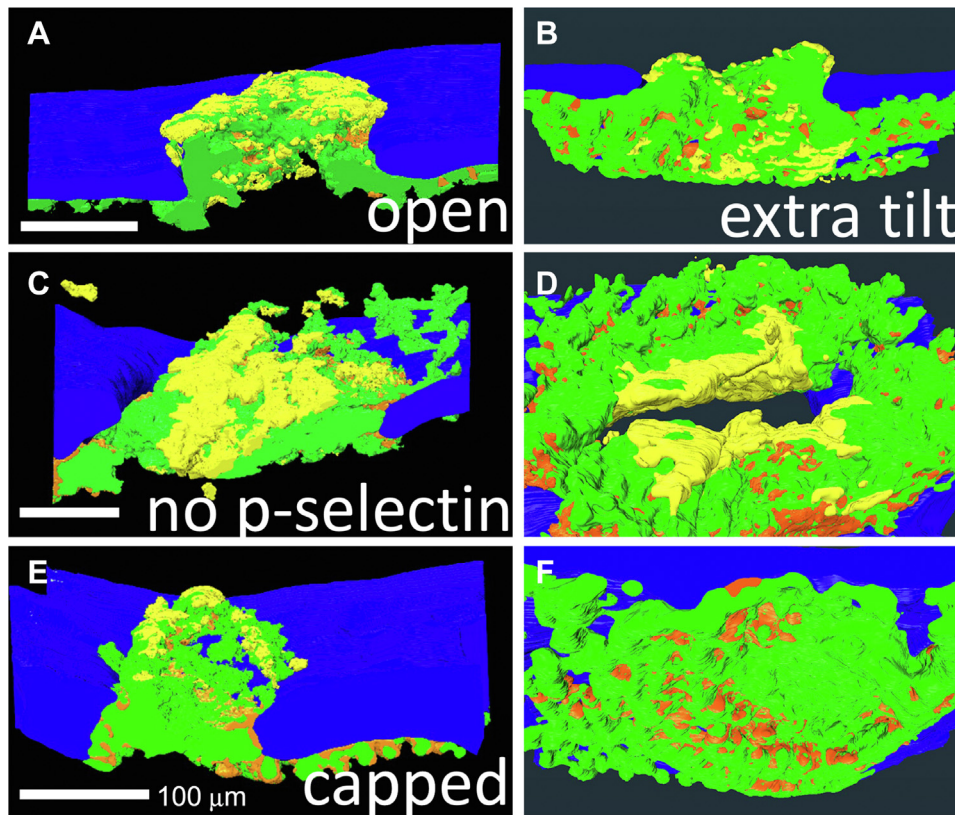
FIGURE 4 Near full thrombus renderings of split open (A, C, E) and extravascular surface (B, D, F) indicating platelet adherence state (loosely adherent to discoid, yellow vs tightly adherent, green) and pockets of highly activated, degranulated platelets (orange). Renderings are from SBF-SEM images (100 nm XY raw pixel size) taken across full thrombus widths every 200 nm. Once the thrombus caps, loosely adherent/ discoid-shaped platelet accumulation is restricted to intravascular accessible thrombus surfaces. A total of four 1-minute point samples were performed for SBF-SEM. In addition, 100 nm XY images were taken every 200 nm across the full thrombus width.

extravascular assembly patches following thrombus closure. This interpretation is supported by a shift in appearance between the thrombus volumes rendered at 1 minute after puncture and at 5 minute after puncture, from a very pebbly extravascular surface at 1 minute indicative of multiple assembly patches to the smoother surface at 5 minutes (Supplementary Figure 2).

3.2 | The decline in assembly patch incidence as thrombus growth slows and platelet activation state patterning shifts suggests a cellular basis for limiting thrombus growth

Next, we tested a prediction for self-limiting thrombus growth, ie, if discoid platelet tethering and assembly patch formation is the basis of thrombus growth propagation, then the occurrence of assembly patches should be inversely correlated with the rate of thrombus growth. As shown both qualitatively and quantitatively (Figures 5 and 6), thrombus growth patterns changed profoundly between 1 minute and 20 minutes; measured platelet volume and total thrombus volume trended toward a peak at approximately 5 minutes after puncture ($P = .33$, 1 minute vs 5 minutes) with evidence of contraction by 20 minutes after puncture. Qualitatively and quantitatively, the contribution of

intrathrombus vaulting to thrombus volume was greatest at 5 minutes after puncture (Figures 5 and 6A, $P < .05$). At both 5 and 20 minutes after puncture, our images showed little to no evidence for platelet accumulation within the vaulted portions of the intravascular thrombus crowns (Figure 5B, C). At 5 minutes after puncture, there was variable sheathing of the intravascular surface of the thrombus with rounded, loosely adherent platelets (Figures 5B and 6F, $P < .05$). At 20 minutes after puncture, loosely packed, predominantly rounded platelets were decidedly enriched in the peripheral intravascular sheath of the thrombus crown (Figures 5C and 6F, $P < .001$). Quantitatively, the extravascular volume of accumulated platelets trended over time to increase despite the fact that this region of the thrombus had no direct access to circulating platelets within the vessel lumen at 5 or 20 minutes after puncture (Figure 6B, $P = .30$). As shown in Figure 6D, E, the extravascular volume portion of degranulated and tightly adherent increased with time, in particular, between 5 and 20 minutes ($P < .05$), whereas loosely adherent platelets had the opposite outcome, increasing intravascularly (Figure 6F, $P < .05$). Note: Extravascular platelet accumulation is underestimated because the sequential sectioning area was limited to approximately 500 μm by 300 μm. Significantly, at each time point, the most numerous platelet activation state was tightly adherent (Figure 6C, $P < .05$).

A 1 min post puncture

B 5 min

C 20 min

50 μm bar
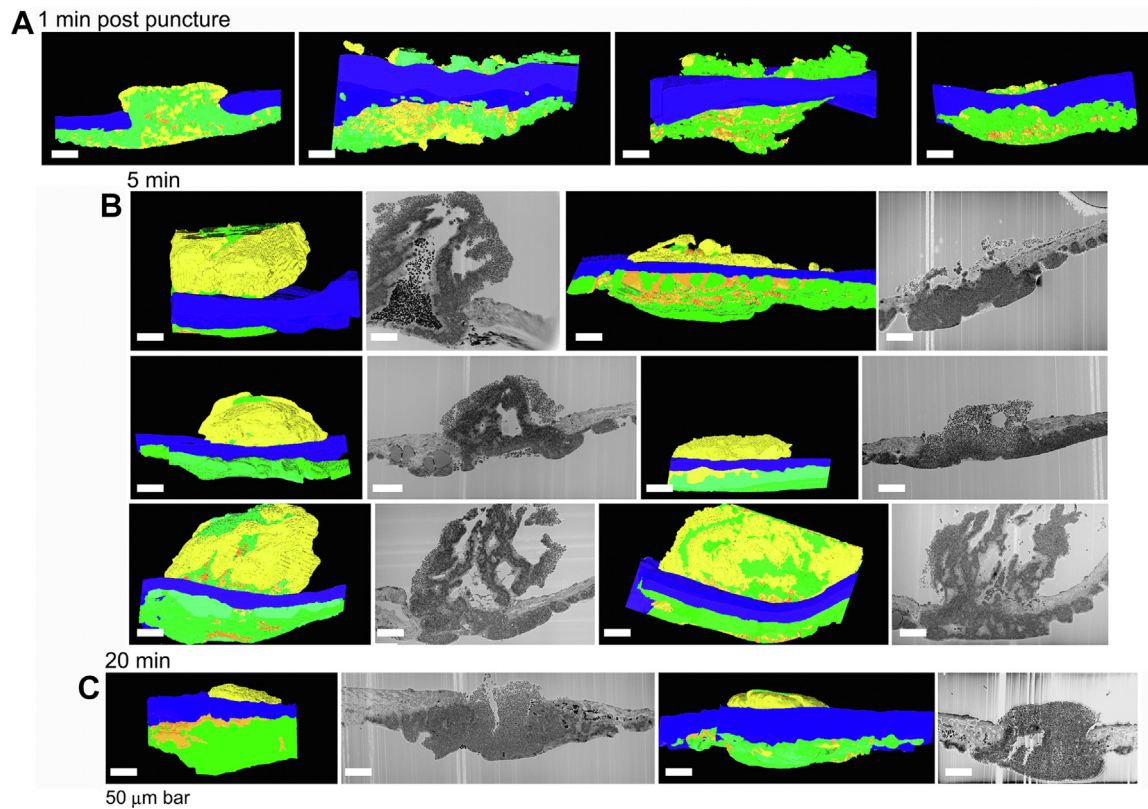
FIGURE 5 Side-viewed renderings (A. 1-minute, one-split open example) and thrombus cross section slice as a raw micrograph and side-viewed renderings (B. 5 minutes and C. 20 minutes) of all SBF-SEM imaged samples. SBF-SEM images were collected across full thrombus width every 200 nm. Raw SBF-SEM micrographs for 1-minute thrombi are shown in Figure 3. Loosely adherent extravascular platelets in these side-view renderings are only seen in the 5- and 20-minute examples when such areas extend into the puncture hole. Color coding: loosely adherent to discoid, yellow vs tightly adherent, green and pockets of highly activated, degranulated platelets, orange. Activation-based segmentation and renderings are from SBF-SEM images (100 nm XY raw pixel size) taken across full thrombus widths every 200 nm. Once the thrombus caps, loosely adherent/discoid-shaped platelet accumulation is restricted to intravascular accessible thrombus surfaces. For more detail, please see [1]. Total number of SBF-SEM samples shown for each time postpuncture wounding.

As macrothrombus growth slows or ceases, does circulating platelet recruitment to the thrombus stop? To resolve this question, the full set of SBF-SEM images acquired with a 100-nm pixel size and spaced in Z by 200 nm and the higher magnification images acquired with a 20-nm pixel were displayed and inspected on a high-resolution computer screen. As shown in Figure 7B, D, the asterisks denote 2× zooms of the boxed areas in A and C, rare assembly patches containing a few discoid-shaped platelets were detected in a downstream area of the thrombus crown. In thrombi at 5 minutes after puncture, these assembly patches were located at the tips of loosely packed, intravascular platelet sheaths (Figure 7A, B), which show midthrombus and intravascular rendered thumbnail views of one such 5-minute thrombus, and in thrombi, at 20 minutes after puncture, the assembly patches were found at the flow distal periphery of the loosely adherent sheath (Figure 7C, D). Surprisingly, these results indicate that a low level of circulating platelet capture is still occurring even at 20 minutes after puncture. We suggest overall that these results could be explained on the basis of decreased signaling intensity over time rather than a qualitative shift in signals with time. Our results in the next section show that both $P2Y_{12}$ and thrombin signaling are required early in thrombus formation, a result consistent with multiple signals acting early. Note that as shown in Supplementary Figure 3, flow produced a variable effect on intravascular platelet accumulation, ie, skewing, at an early time point with accumulation on the upstream side being relatively high, a trend reversed at 5 minutes and was balanced with upstream and downstream at 20 min.

3.3 | Treatment with the direct-acting inhibitors, dabigatran, and cangrelor indicates that multiple signaling pathways act early and produce differential outcomes

Earlier work has shown that a direct-acting $P2Y_{12}$ receptor inhibitor such as cangrelor can delay thrombus formation as early as 5 minutes after puncture in a mouse jugular vein model [1,4], whereas thrombin has important known early effects on thrombus formation and later effects on jugular vein thrombus formation [1,17]. We speculated that both $P2Y_{12}$ and thrombin, known protease activators of PAR receptors, might be acting early in thrombus formation, and hence, pretreatment with the respective inhibitor might reveal important
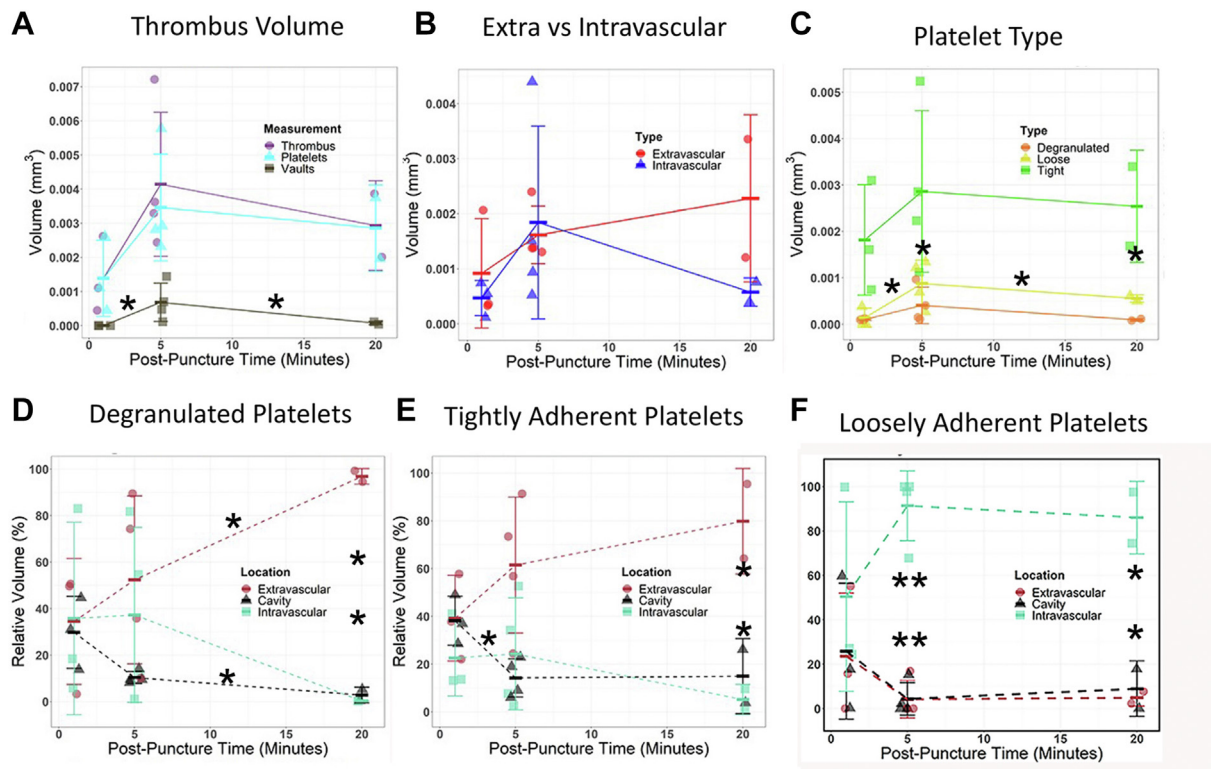
FIGURE 6 Quantitation of thrombus formation parameters: volume, extravascular vs intravascular platelet distribution, platelet type, and relative volume % of degranulated platelets, tightly adherent platelets, and loosely adherent platelets within the total thrombus volume sectioned. Intravascular thrombus volume appeared to peak at 5 minutes after puncture, whereas the extravascular volume continued to increase. The portion of a given platelet activation type that was extravascular increased over time. The data were derived from the segmentation, rendering and quantification of the examples shown in Figure 5. P value comparisons with a value of <.05 are indicated with an * and those with a value of < .001 are indicated with a **. P indicators placed on the graph indicate significant time series events, and those placed vertically, between data points, indicate significant differences in location or between platelet activation type at a given time point. Dot plots include the total sample sets performed.

signaling requirements for initial platelet anchoring, degranulation, and tethering during thrombus formation.

As expected from our previously published results [1], pretreatment with the DOAC, dabigatran, a thrombin inhibitor at a concentration sufficient to produce a mild bleeding defect in mice [1], resulted in a capped 5-minute thrombus that was heavily enriched in tightly adherent platelets (Figure 8A). Significantly when platelet activation was examined at high zoom in the WA-TEM images of the adventitia/thrombus interface, the platelets within a short distance of <5 microns of this collagen demarcated interface failed to show severe degranulation accompanied by the loss of cytosol (Figure 8B). This is a striking difference relative to the very obvious degranulation and cytosol loss seen in control (Figures 1–3). Thrombin-dependent platelet activation at this interface is not surprising. What is surprising is that this failure to produce a high degree of platelet activation has at most a mild bleeding effect.

On the other hand, cangrelor pretreatment at a concentration sufficient to produce a bleeding defect [1,4] yielded an uncapped, open 5-minute thrombus that appeared stalled in its formation at a point resembling an early 1-minute thrombus (compare Figure 8C with Figure 2A). Remarkably, the cangrelor pretreated thrombus showed

significant examples of peripheral, tethered, discoid platelet strings, and all other platelet activation phenotypes. This suggests that P2Y$_{12}$ is required in general for the rapid propagation of thrombus formation and the sequential conversion of circulating platelets to tightly adherent platelets. Specifically, there was no apparent inhibition of platelet degranulation and cytosol loss at the adventitia/thrombus interface (Figure 8D) providing explicit evidence that this process is selectively dependent on thrombin signaling. Importantly, because cangrelor produces a strong inhibition of thrombus propagation, this led us to examine whether there was direct tethering of discoid platelet strings to the adventitia. As shown in Figure 8E, platelet string anchoring was not to the adventitia but rather to a highly activated, degranulated, cytosol-depleted, thin layer of discoid platelets. These adherent, near "platelet ghosts" appeared flattened (Figure 8E, Supplementary Figure 4). The data suggest that initial platelet anchoring is the result of direct interactions between circulating platelets and exposed collagen or other adventitial proteins, see Figure 8F for a schematic Tethered Capture and Activate model. That circulating platelet recruitment is of very low activation state platelets is consistent with the occurrence of dense granules in the discoid platelet examples shown in Figure 8E and especially Supplementary Figure 4.
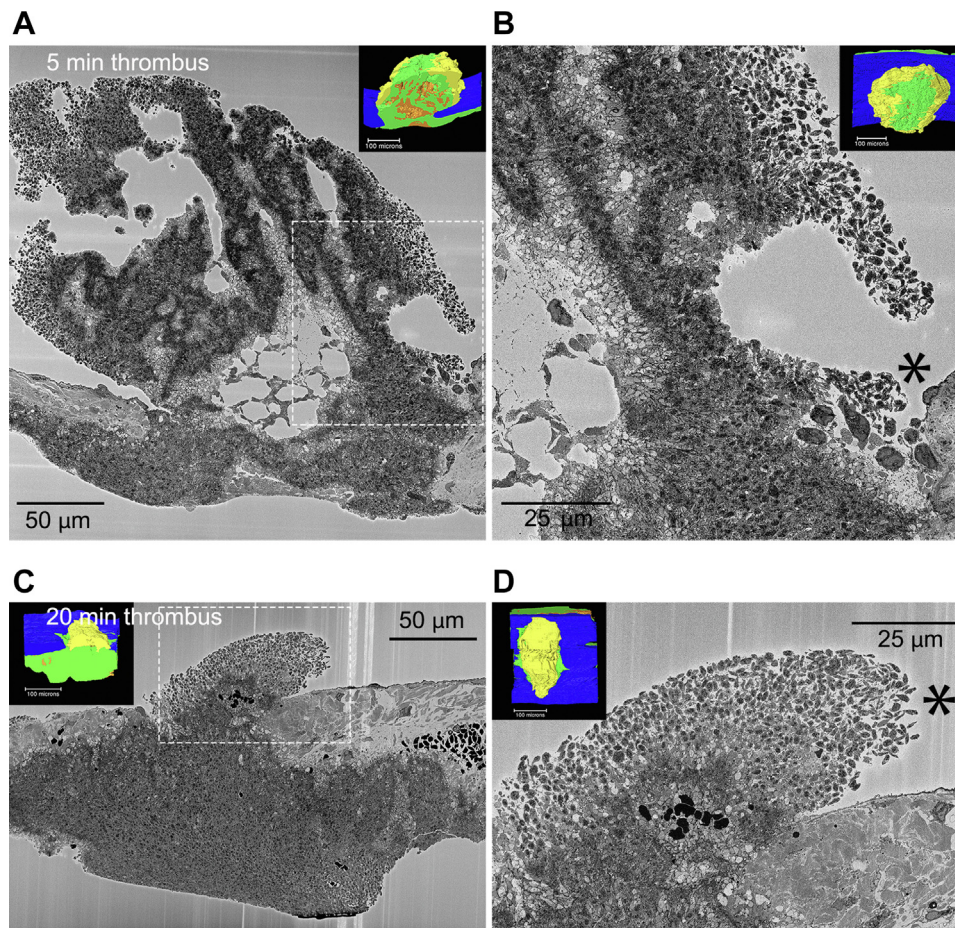
FIGURE 7 Peripheral, discoid platelet accumulation in 5- (A,B) and 20-minute (C,D) thrombi is restricted to small, flow protected patches. A, C) near full thrombi cross sections. B, D) 2× higher zoom of downstream protected areas. Dashed boxes mark areas of peripheral, discoid-shaped platelet accumulation. Insets show the overall thrombus arrangement as rendered from 2000 to 2500 images spaced 200 nm apart. Yellow, loosely adherent platelets; green, tightly adherent platelets; orange, stripes of highly degranulated, procoagulant-like platelets. Images from SBF-SEM micrographs, 20 nm raw pixel size. Five-minute postpuncture, $N = 6$; 20-minute postpuncture, $N = 2$.

In conclusion, the data indicate the following 3 separate forms of circulating platelet recruitment to the exposed, damage area: (1) direct anchoring of discoid platelets to the adventitia and subsequent in situ activation, (2) platelet/platelet string tethering to the highly activated, adventitia, and presumably collagen-anchored platelet layer, and (3) platelet/platelet string tethering to peripheral, loosely adherent platelets. Presumably, because the activation state of the recipient thrombus bound platelet in each case is different, the underlying mechanisms could well be different.

4 | DISCUSSION

We present ultrastructure evidence for multiple mechanisms of circulating platelet capture within a puncture wound. These include both direct capture of discoid circulating platelets to the exposed collagen-rich adventitia, the local tethering of circulating platelets to highly activated, adventitial anchored platelets, both key steps in thrombus initiation, and the tethering of circulating platelets to less

activated, peripheral platelets to produce a progressive "assembly patch" in which platelet capture is coupled to subsequent platelet activation, key steps in thrombus propagation. We propose here that tethered circulating platelet capture provides a general mechanism for restricting platelet activation to the immediate site of endothelial damage. We define circulating platelet tethering as the gapped retention, be it 50 nm or more, of individual platelets or multiple platelet long strings in which the individual discoid platelets present the morphological properties of circulating platelets including shape, the lack of pseudopod extensions, and the presence of α-granules and dense granules. These platelets display no structural evidence of activation. Because they are physically restricted to the immediate site of vascular damage as evidenced by retention during the preparative procedure, any subsequent activation step will occur within the spatial confinement of the thrombus. These activation steps generate the surface for sequential rounds of platelet tethering and thrombus growth as summarized in a Tethered Capture and Activate model (Figure 8F). We submit that our ability to reveal these outcomes is only possible because of state-of-the-art electron microscopy
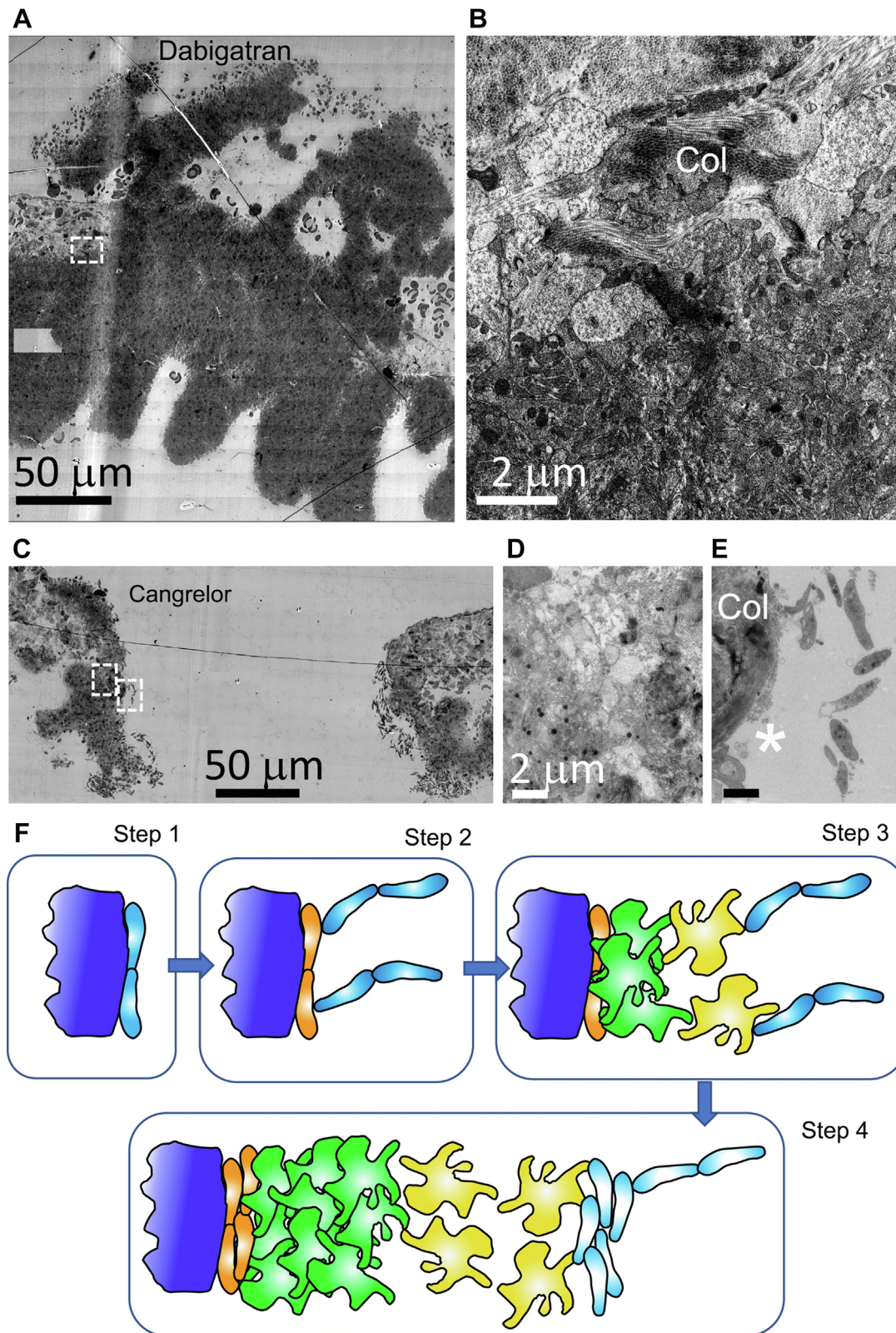
FIGURE 8 The DOAC, dabigatran, and the acute acting, anti-platelet drug, cangrelor, differentially affect puncture wound thrombus formation and platelet activation at the collagen-rich adventitia/thrombus interface. WA-TEM, 3.185 nm XY raw pixel size. A. Overall appearance of a 5-minute postpuncture thrombus from a dabigatran pre-treated mouse. Montaged image, 5-minute postpuncture, approximately mid-thrombus, postbleeding cessation. The thrombus consisted mainly of tightly adherent platelets with limited intravascular accumulation of loosely adherent platelets. Vessel walls are to the left and right of the thrombus. Top, intravascular and bottom, extravascular. B. Zoom of collagen/platelet interface of dabigatran treated jugular thrombus (dashed box in A). The platelets at the interface possess are

automation that permits visualization from the nm scale to the near millimeter scale of a puncture wound thrombus.

We propose that the Tethered Capture and Activate model described above carries within it an implied mechanism for limiting puncture wound growth. Assuming local signals of short life times, thrombus growth would be limited to the immediate injury site, the qualitative nature of the signal and by the strength of the signal, ie, intensity. Because both a $P2Y_{12}$ receptor inhibitor, cangrelor, and a DOAC, dabigatran, affected early steps in jugular vein puncture wound formation, within 5 minutes or less, one is forced to conclude that multiple signaling pathways act in parallel during thrombus formation, indicating that sequential timing of signaling pathways, PAR vs $P2Y_{12}$ receptor as previously suggested, is an unlikely explanation for changes in accumulated platelet morphology at 1 minute after puncture vs 5 minutes or later, eg, 20 minutes. Our data indicate that thrombus volume growth in the jugular puncture wound had significantly slowed or even stopped by 5 minutes after puncture. Consistent with that observation, the intravascular occurrence of tethered discoid platelets declined to being almost undetectable at 5 minutes after puncture. We propose that this decline in tethered platelets can be explained by a decrease in signal intensity that leads to increased intravascular accumulation of loosely adherent platelets within a contracted 20-minute thrombus.

Tethered Capture of circulating platelets to different activation states suggests the possibility of context sensitive molecular interactions. At present, any suggestion for the molecular basis of platelet tethering is speculative. One logical candidate protein is VWF and its elongated multimers. VWF-mediated platelet interactions with activated endothelial cells are a well-studied case. In this case, VWF bridges between endothelial cells and platelets through electrostatic interactions with the damaged endothelium and binding to platelet GP1bα (eg, [17]). Within a wound, one might propose that activated platelet adherent VWF could act as the fishing line for circulating platelet recruitment to the growing thrombus. The protease ADAMTS13 might then downregulate VWF, eg, [18], ie, decreased signal intensity, and bring a severe decline in circulating platelet capture. We submit that the present case could provide a normal function for VWF platelet strings in a healthy person (see [19] for review). Further research beyond the scope of the present study will be required to test this or any other hypothesis regarding a detailed role of VWF in the forming puncture wound thrombus.

Our results raise questions about the relative importance of diffusible and contact signals in thrombus formation and the spatial distances over which they act. Perhaps surprisingly, we found that discoid platelet tethering to a thin, adventitial anchored platelet patch did not lead to immediate activation of adjacent tethered platelets even though separation distances were small, no more than 40 to 50 nm in the nearest cases. Discoid platelet shape was at least transiently maintained, and dense granules could be readily identified in the sections. A similar question applies to peripheral discoid-shaped platelet tethering and platelet activation as the thrombus grows. Distinct layering of platelet activation was seen over distances as small as 5 μm or less. At the periphery, platelets were very discoid; at a distance of 1 μm, inward extended pseudopods emerged as distinctive platelet features, and slightly more inward platelets became rounded and within 5 μm of the periphery tightly adherent. In brief, any diffusible signaling is apt to be quite local and is probably influenced by flow (Figure 2). Certainly, outward blood flow through the puncture provides the simplest explanation for the flow-parallel discoid platelet arrangement. The present results point strongly to progressive platelet activation in 3D space and the consequent, stepwise movement of platelet recruitment further and further from the exposed adventitia. It suggests that granule secretion, in particular, that of ADP or other small molecules from dense granules, should

---

degranulated with a cytoplasm/cytosol rich in proteins and hence one that has electron density. Control, 5-minute, WT platelets show both degranulation and extensive cytosol loss at the adventitial interface (Figure 7B, see also [1] ie, dabigatran-inhibited cytosol loss. C. 5-minute cangrelor-treated thrombus showing abundant peripheral, discoid-shaped platelets and progressive increase in apparent activation state within the thrombus. Left and right boxes in (C) mark the position of adventitial interface (left box) and a platelet string (right box) shown at higher zoom in (E). D. Frame showing that cangrelor has little to no inhibitory effect on platelet degranulation/cytosol loss at the collagen/platelet interface. E. Zoom of platelet string at position marked by right box in (C). The string is tethered to a thin collagen anchored platelet layer (white asterisks, see also Supplementary Figure 4). In both cangrelor and dabigatran platelets, rounded, darkly staining mitochondria were the prominent cytosolic organelle. Col, collagen. F. Tethered Capture and Activate Model for platelet recruitment in a venous puncture wound thrombus. Step (1)—early discoid platelet recruitment/capture to generate a monolayer of discoid platelets (light blue) directly bound to adventitia (dark blue). An important role for collagen and GPVI as the major collagen receptor is postulated. Collagen bound VWF may also be contributory; step (2)—initial platelet anchoring directly to collagen leads to extensive platelet degranulation and cytosol loss and subsequent step 2 capture of discoid platelet strings is to the thin layer of degranulated platelets (orange). Step (3)—discoid platelets rapidly convert to loosely adherent (yellow) and tightly adherent (green) platelets. As shown in step 3, subsequent capture of discoid platelet strings to loosely attached platelets. Circulating platelet capture in steps 3 and 4 lead to the formation of platelet pedestals and columns within the growing thrombus. Step (4)—repeated rounds of discoid platelet recruitment with conversion to loosely adherent platelets and tightly adherent platelets accompanied by some increase in the number of degranulated platelets at the adventitial interface leads to full thrombus formation. Note that in this model, both thrombin and $P2Y_{12}$ signaling happen early and are rate contributing. The data suggest that there is no qualitative change in molecular signaling but rather a decrease in the signaling intensity with time. Whether discoid platelet, ie, circulating platelet capture to different surfaces occurs through identical molecular mechanisms is an open question to be addressed in future experimentation. Consistent with previous literature, we propose that VWF is the likely long tethering protein involved in the formation of platelet strings. Dabigatran – WA-TEM concentration series of 15 mg/kg, 50 mg/kg, and 150 mg/kg dabigatran was performed with 2 to 3 samples at each concentration. N = 3 at 150 mg/kg dabigatran. Cangrelor – Concentration per Materials and Methods. N = 2.

occur in a "frontal" manner as a wave(s) of platelet activation tracks forward with the peripheral recruitment and tethering of circulating platelets to the growing thrombus. This is a putative feature of platelet signaling within the growing thrombus not considered in the consensus Core and Shell paradigm [4,20]. In that paradigm, platelets are considered to be almost binary in their activation state, spatial distribution, and secretion properties. In contrast, the highly localized thrombus propagation observed in the jugular vein thrombus model is consistent with the recently proposed Cap and Build paradigm of thrombus formation [21].

We probed in detail how $P2Y_{12}$ and thrombin inhibition affected accumulation of procoagulant-like platelets at the adventitia/thrombus interface. Cangrelor had little to no effect on the accumulation of procoagulant-like platelets at the adventitial interface. In contrast, dabigatran inhibited the cytoplasm loss/blebbing characteristic of procoagulant platelet formation. One interpretation is that $P2Y_{12}$ receptors are not important early. However, that interpretation is refuted by the fact that cangrelor in drug pretreated mice stalled thrombus formation early. In brief, our data strongly indicate that both thrombin- and $P2Y_{12}$-dependent systems are co-active early in thrombus formation. Moreover, the early thrombus formation importance of a $P2Y_{12}$ inhibitor is totally consistent with previous publications that mutations affecting dense granule biogenesis and/or release cause pronounced bleeding defects [22].

More puzzling and more difficult to explain is the global differences in platelet activation state apparent in the cangrelor and dabigatran-pretreated thrombi 5 minutes after puncture. In the cangrelor case, the thrombus displayed a diverse range of platelet activation states arranged in a manner consistent with a Capture and Activate model. In contrast, dabigatran-pretreated thrombi displayed little diversity in platelet activation state; most platelets were tightly adherent. These differences were true even through functionally, the $P2Y_{12}$ inhibitor effect was stronger; bleeding continued and little extravasvascular capping of the wound was apparent. In the antithrombin case, bleeding had ceased and the puncture hole was capped extravascularly. One plausible explanation for the differences is that a multiplicity of signaling pathways is needed to give a normal outcome. Perhaps more interesting is the possibility that this contrast illustrates that there is some redundancy in steps and that, in the dabigatran case, a core set of functions essential to bleeding cessation is retained. Structurally, this outcome is consistent with platelet adhesion, presumably integrin mediated, being essential. If so, one could interpret the outcome as suggesting any decrease in $P2Y_{12}$ receptor contribution to platelet adhesion is uniquely a risk factor. We note that these outcomes only became apparent because of new cangrelor data and present data mining approaches.

In total, we propose that our analysis suggests a new perspective on how self-limiting thrombus growth occurs. All events observed here, at a subplatelet detail, from initial platelet anchoring to the exposed adventitia, circulating platelet tethering/capture and progressive platelet activation within the thrombus occur locally. Moreover, these experiments begin to place limits on the signaling processes involved. First, considering the very short distances over which platelet activation outcomes were observed, any diffusible signals involved are likely to be spatially restricted, short lived, or rapidly diluted by flow. Second, our inhibitor results indicate that signal systems co-act in time and likely space. Although not part of previous paradigms, this outcome is hardly surprising, considering the number of receptor systems present on the platelet surface. Third, our inhibitor experiments point to the accumulation of a single platelet activation class, ie, tightly adherent platelets, as being central to bleeding cessation and a potential drug risk factor. Fourth, our experiments suggest that a reduction in signaling intensity is a key limiting factor in regulating thrombus growth. In brief, we submit that these outcomes are significant clinically because they point to distinct platelet activation states that may be susceptible to therapeutic control, and on the other hand, the states might be preferential risk factors. Our results provide evidence that current antiplatelet and anticoagulation factor drugs can act in a manner hitherto unexpected. Furthermore, the methodology itself has the potential to become a new gold standard for probing drug action and consequences.

AUTHOR CONTRIBUTIONS

I.P. and S.R. contributed equally to experimental implementation with major roles in data gathering. K.B. was responsible for puncture wounds and all animal surgeries at UAMS. J.K. supported electron microscope sample preparation and electron microscopy at UAMS. All SBF-SEM was performed by the Leapman laboratory at NIH, NIBIB with O.Z., D.C., and J.C. responsible for experimental implementation/data analysis steps and M.A.A. and R.L. being major contributors to experimental design and supervision. I.P. was the lead person for all electron microscope sample preparation and WA-TEM. I.P. was responsible for data validation and coordination between the Storrie and Leapman laboratories. R.L., S.R., and B.S. had major responsibilities for experimental design, data quality control, and manuscript preparation. B.S. prepared the first draft and took senior author responsibility for seeing the manuscript through to completion. All authors read and approved the final version of the paper.

RELATIONSHIP DISCLOSURE

There are no competing interests to disclose.

ORCID

Brian Storrie https://orcid.org/0000-0002-4644-2504

REFERENCES

[1] Rhee SW, Pokrovskaya ID, Ball KK, Ling K, Vedanaparti Y, Cohen J, et al. Venous puncture wound hemostasis results in a vaulted thrombus structured by locally nucleated platelet aggregates. *Commun Biol.* 2021;4:1090.

[2] Chattaraj SC. Cangrelor AstraZeneca. *Curr Opin Investig Drugs.* 2001;2:250–5.

[3] Eisert W, Hauel N, Stagier J, Wienen W, Clemens A, van Ryn J. Dabigatran: an oral novel potent reversible nonpeptide inhibitor of thrombin. *Arterioscler Thromb Vasc Biol.* 2010;30:1885–9.

[4] Tomaiuolo M, Matzko CN, Poventud-Fuentes I, Weisel JW, Brass LF, Stalker TJ. Interrelationships between structure and function during the hemostatic response to injury. *Proc Natl Acad Sci USA.* 2019;116:2243–52.

[5] Pokrovskaya I, Joshi S, Tobin M, Desai R, Aronova MA, Kamykowski JA, et al. SNARE-dependent membrane fusion initiates α-granule matrix decondensation in mouse platelets. *Blood Adv.* 2018;2:2947–58.

[6] Pokrovskaya ID, Szwedo JW, Goodwin A, Lupashina TV, Nagarajan UM, Lupashin VV. Chlamydia trachomatis hijacks intra-Golgi COG complex-dependent vesicle trafficking pathway. *Cell Microbiol.* 2012;14:656–68.

[7] Holcomb PS, Hoffpuir BK, Hobson MC, Jackson DR. Synaptic inputs compete during rapid formation of the calyx of Held: a new model system for neural development. *J Neurosci.* 2013;33: 12954–69.

[8] Pokrovskaya ID, Yadav S, Rao A, McBride E, Kamykowski JA, Zhang G, et al. 3D ultrastructural analysis of α-granule, dense granule, mitochondria, and canalicular system arrangement in resting human platelets. *Res Pract Thromb Haemost.* 2020;4:72–85.

[9] Pokrovskaya ID, Aronova MA, Kamykowski JA, Prince AA, Hoyne JD, Calco GN, et al. STEM tomography reveals that the canalicular system and alpha-granules remain separate compartments during early secretion stages in blood platelets. *J Thromb Haemost.* 2016;14:572–84.

[10] Becker RC, Sexton T, Smyth SS. Translational implications of platelets as vascular first responders. *Circ Res.* 2018;122:506–22.

[11] Kim D, Ku D. Structure of shear-induced platelet aggregated clot formed in an in vitro atrial thrombosis model. Blood Adv. In press.

[12] Fang J, Hodivala-Dilike K, Johnson BD, Bryon D, Du LM, Hynes RO, et al. Therapeutic expression of the platelet-specific integrin, alphaIIbbeta3, in a murine model for Glanzmann thrombasthenia. *Blood.* 2005;106:2671–9.

[13] Casa LDC, Deaton DH, Ku DN. Role of high shear rate in thrombosis. *J Vasc Surg.* 2015;61:1068–80.

[14] Nolte MA, Margadant C. Activation and suppression of hematopoietic integrins in hemostasis and immunity. *Blood.* 2020;135:7–16.

[15] Kato K, Kanaji T, Russell S, Kunicki TJ, Furihata K, Kanaji S, et al. The contribution of glycoprotein VI to stable platelet adhesion and thrombus formation illustrated by targeted gene deletion. *Blood.* 2003;102:1701–7.

[16] Stalker TJ, Traxler EA, Wu J, Wannemacher KM, Cermignano SL, Voronov R, et al. Hierarchical organization in the hemostatic response and its relationship to the platelet-signaling network. *Blood.* 2013;121:1875–85.

[17] André P, Denis CV, Ware J, Saffaripour S, Hynes RO, Ruggeri ZM, et al. Platelets adhere to and translocate on von Willebrand factor presented by endothelium in stimulated veins. *Blood.* 2000;96:3322–8.

[18] Chauhan AK, Motto DG, Lamb CB, Bergmeier W, Dockal M, Plaimauer B, et al. Systemic antithrombotic effects of ADAMTS13. *J Exp Med.* 2006;203:767–76.

[19] De Ceunynck K, De Meyer SF. Vanhoorelbeke. Unwinding the von Willebrand factor strings puzzle. *Blood.* 2013;121:270–7.

[20] Stalker TJ, Welsh JD, Brass LF. Shaping the platelet response to vascular injury. *Cur Opin Hematol.* 2014;21:410–7.

[21] Brass LF, Diamond SL, Stalker TJ. Platelets and hemostasis: a new perspective on an old subject. *Blood Adv.* 2016;1:5–9.

[22] Nurden AT, Freson K, Seligsohn U. Inherited platelet disorders. *Haemophilia.* 2012;18:154–60.

SUPPLEMENTARY MATERIAL

The online version contains supplementary material available at https://doi.org/10.1016/j.rpth.2023.100058